Anzhu Chen
Master of Engineering, *orcid.org/0000-0002-6022-9793*
Yancheng Polytechnic College, School of Automotive Engineering, Yancheng 224005, China
Pengfei Zhou
Master of Engineering, *orcid.org/0000-0002-5459-9130*
Yancheng Polytechnic College, School of Automotive Engineering, Yancheng 224005, China;
Soochow University, Shagang School of Iron and Steel, Suzhou Jiangsu 215137, China;
Jiangsu delonyc Electromechanical Technology Co., Ltd. Jianhu Jiangsu 224731, China

THE INVESTIGATION OF EUTECTIC NUCLEATION AND GROWTH MECHANISM OF AL-SI ALLOY

Abstract. *Al-Si binary eutectic transformation, solidification occurred in the late eutectic (cell) crystal nucleation, eutectic nucleation and growth are a direct impact on formation of the defects of organizations (such as: shrinkage, thermal cracking, etc.) and the distribution of impurities elements and compounds, and so on .In this paper, analysis the microstructure of the alloy with modification by Sr, also thermal analysis was used to measure the unmodified alloys, EBSD was used to analysis the alloy with different status. The results showed that: The EBSD technique, whether or not modification, we observed that the eutectic nucleation on the primary dendrite and heterogeneity in inter-dendrites exist, and Sr has a significant effect on the primary α-Al, the primary α-Al phase in the AlSi10.5 alloy modified by 0.04% Al-10 wt. % Sr is more rounded and the size is much smaller than unmodified alloy. Fe has a great influence on the nucleation of eutectic Si.*

Keywords: Al-Si alloy; EBSD; Eutectic Nucleation

Introduction

Aluminum alloy has small density, good plasticity, excellent electrical conductivity and thermal conductivity. It has a dense oxide film on the surface to play a protective role, good corrosion resistance and can be recycled and reused. It is a green and sustainable development Non-ferrous metal. Therefore, aluminum alloys are widely used in aerospace, automotive, high-voltage transmission equipment and other fields [1-3]. Al-Si alloys can obtain partial or complete eutectic structure depending on the composition of alloy or the change of solidification conditions. The solidification process has always been a topic of great interest to researchers [4-7]. The volume fraction of the (α+Si) eutectic is approximately 50% to 90%. Except for the primary crystal (α-Al or Si phase) in the Al-Si alloy structure, the volume fraction, morphology, number and distribution of the eutectic are significant influences the microstructure and mechanical properties of the alloy.

Since the growth rate of the leading eutectic Si phase is greater than the growth rate of the eutectic α phase, it can penetrate into adjacent eutectic (cluster) grains or dendritic α-Al phases during the growth process, making the final solidification. The eutectic grain boundaries and the grain boundaries of the eutectic and primary dendrite α-Al (hypoeutectic) are interleaved with each other, and the true grain boundary cannot be judged [6-15]. Therefore, under the general optical microscope (OM), only the overall characteristics of the eutectic structure can be observed, and the size、number and morphology of the eutectic (cluster) grains cannot be judged. This is an in-depth study of the shape of the eutectic (cluster) grains. Nucleus and growth bring certain difficulties. Although transmission electron microscope (TEM) can analyze the orientation relationship between two phases in detail, it is difficult to fully reflect the characteristics of the eutectic structure due to the small field of view observed. A K Dahle [7] analyzed eutectic nucleation and growth problems based on EBSD (Electron backscatter diffraction) images; D Stuart et al. [13] used high-purity and industrial pure Al-10%Si alloys (without deterioration) as the research object, using liquid quenching (in the eutectic transition) process and normal solidification (average cooling rate of 1.5 °C/s, respectively). Under the conditions of the macroscopic and microscopic organization, the results show that: The impurity elements in the alloy have a great influence on the morphology and size of the eutectic grains, but they do not give a clear explanation; S Shankar [14] studied eutectic nucleation problem of ultra-high purity Al-7%Si by means of SEM、TEM, etc.

Since the Al-Si binary eutectic transformation takes place in the late stage of solidification, its nucleation and growth behavior all directly affect the formation of defects such as shrinkage as well as the distribution of precipitated phases and impurity elements. Japanese

scholar Ohno Naomi pointed out that the mechanical properties of eutectic (near eutectic) alloys depend not only on the primary microstructure and the eutectic microstructure, but also on the grain boundaries of eutectic (cluster) grains. Obviously, to clarify the formation mechanism of eutectic (cluster) grains and find ways to control the morphology and size of eutectic (cluster) grains is obviously important for improving the performance of (near) eutectic alloys. Therefore, in this paper, the microstructure of AlSi10.5 alloys in both metamorphic and non-metamorphic states is studied. The nucleation and growth characteristics of eutectic (cluster) bodies during the solidification process are revealed by thermal analysis without metamorphism, and the nucleation law of nondeforming is analyzed by EBSD techniques.

Experimental procedure

The test material is an AlSi10.5 alloy, and its chemical composition is shown in Table 1. The Al-10 wt. % Sr aluminum was used as a modifier, and the chemical composition is shown in Table 2.

Table.1 Chemical composition of AlSi10.5 alloy (wt. %)

Si	Fe	Cu	Mn	Cr	其它	Al
10.2	0.2	＜0.01	＜0.01	＜0.01	＜0.05	余量

Table.2 Chemical composition of Al-10 wt. % Sr alloy (wt. %)

Sr	Fe	Cu	Ti	Mn	Zn	Al
9.76	＜0.02	＜0.01	＜0.01	＜0.01	＜0.05	余量

Two sets of samples were prepared in this test, which were non-degraded samples and metamorphic samples. Sample preparation is as follows:

(1) Non-deteriorating sample: Before smelting, take 2 kg of AlSi10.5 raw material into the crucible, then put the crucible into GR2-5-10 well type crucible melting aluminum furnace; when the temperature to 750°C then the heating is stopped, hexachloroethane is used for degassing and slagging, and the molten aluminum is allowed to stand for 20 min until the aluminum liquid is cooled to 730 °C and cast into a metal mold of φ22 mm×45 mm. The preheating temperature of the metal mold is 200 °C.

(2) Deteriorating sample: According to the smelting step of the non-degraded sample, first melt 2 kg of AlSi10.5. When the temperature of the molten aluminum reaches 750 °C, use hexachloroethane to degas the slag, and wrap it with aluminum foil 0. 4% Al-10 wt. % Sr modifier is pressed into the aluminum liquid and fully stirred. The liquid aluminum is allowed to stand for 20 min until the aluminum liquid is cooled to 730 °C and cast into a metal mold of φ22 mm × 45 mm. heat the mold to 200°C.

Metallographic analysis of non-degraded samples and metamorphic samples; DSC analysis of non-degraded samples; SEM and EBSD analysis of non-metamorphic and metamorphic samples.

Results and Discussion

Alloy microstructure analysis

Figure 1 is a microstructure of a modified and unmodified AlSi10.5 alloy. From Fig. 1(a), it can be seen that the primary α-Al dendrite of the undeformed alloy is coarse and has a diameter of about 50-300 um. After the addition of Sr, the primary α-Al is changed from undenatured dendrite to near-spherical. The size is about 20-40 um, as shown in Figure 1(b).

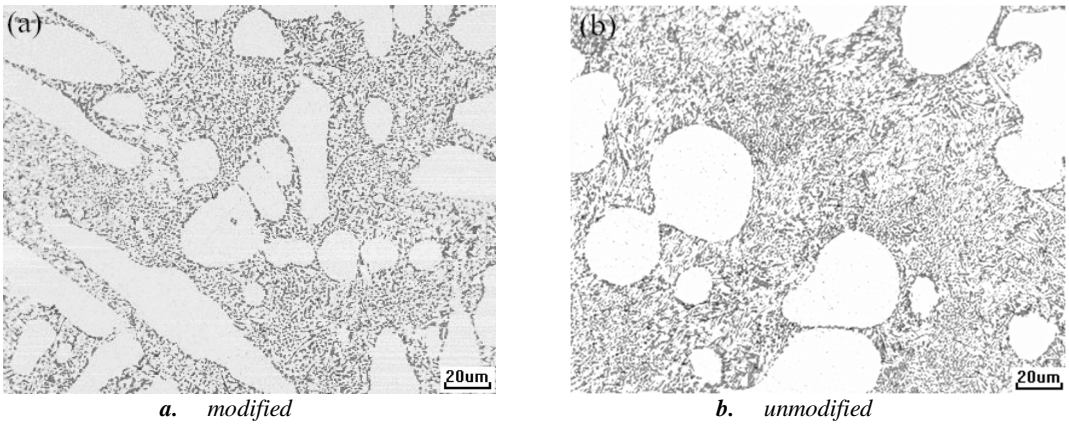

a. *modified* ***b.*** *unmodified*

Figure 1 – Microstructure of alloy

Thermal Analysis of Non-deformed AlSi10.5 Alloy

The thermal analysis method is currently the most effective means to study the refinement, modification and prediction of melt processing quality of Al-Si alloy melts. Thermal analysis is a reflection of the interrelationship between latent heat of phase change during the solidification process and external heat dissipation of the system. From the thermal analysis curve, the precipitation temperature and time of the phase in the solidification process can be obtained.

Figure 2 shows the thermal analysis of an unmodified AlSi10.5 alloy. The dT/dt curve reflects the change of the cooling rate with time, and can better reflect the nucleation and growth of the phase in the solidification process. The point A to point N in the figure is the precipitation of the primary dendrite α-Al phase; as the primary dendriteα-Al phase begins to precipitate, $\left|dT/dt\right|$ changes over time to the zero line, $\left|dT/dt\right| = 0$, that is, point B in the figure, indicating that in this process, a large number of α-Al phases of primary dendrite are precipitated and the system is momentarily balanced. Point B to point P, $\left|dT/dt\right|$ increase with time ($\left|dT/dt\right| \approx 0.38$), indicating that the latent heat of phase change is relatively less, and the precipitation of primary dendriteα-Al phase is smaller than before. Its growth has entered the middle and late stages. It is worth noting that, between PQ, $\left|dT/dt\right|$ approaches the zero line again (that is, the latent heat of phase change slightly increases). This indicates that in the PQ segment, besides the precipitation of the primary dendriteα-Al phase, there must be new phase is precipitated and grown. As far as the composition of the alloy is concerned, the main impurity element is Fe, and it can be considered that the new precipitated phase is mainly a Fe-rich phase precipitated before the pre-eutectic. The NG section is a large number of eutectic nucleation processes. Point N is the eutectic nucleation temperature T_N; point M is the eutectic retinal (T_{Min}) temperature. The eutectic nucleation temperature T_N and the eutectic growth temperature T_G are the first extraordinary change points of the dT/dt curve before and after the re-growth temperature T_{Min}, and correspond to the T-t curve to find the corresponding eutectic transition characteristic temperature. At the beginning of the eutectic growth temperature (i.e., point G, T_G), a slight increase in temperature was observed at T-t, indicating that a large number of nuclei formed at the eutectic stage began to grow; A eutectic plateau then emerged, and the latent heat of phase transition from eutectic precipitation and the heat dissipation of the system reached a dynamic equilibrium. The results of thermal analysis indicate that the Fe-rich phase in the melt may have a great influence on the nucleation behavior of eutectic Si.

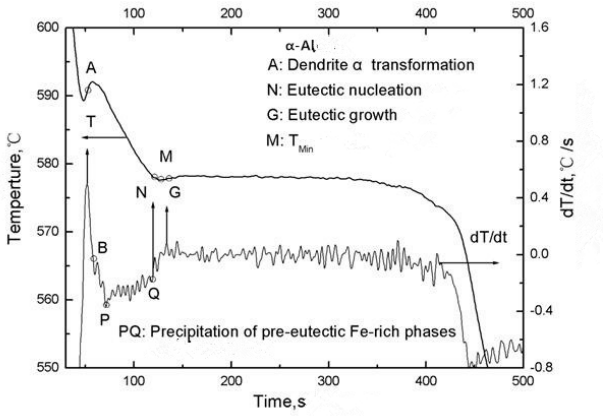

Figure 2 – The curve of thermal analysis of AlSi10.5 with unmodified

EBSD Analysis of Unreformed and Modified Alloys

Figure 3 shows the SEM morphology and EBSD analysis of unmodified AlSi10.5 alloy. It can be seen from the figure that comparing the different eutectic regions indicated by lines 1 and 2, the line 1 area is white, which means that this area (same color) may be the same eutectic group. The same line 2 is pink, and this area may also be the same eutectic group. The eutectic group (including eutectic silicon clusters formed by its frequent bifurcation) refers to a region composed of a eutectic Si grown from a nucleus and α phase coupled thereto. In the non-altered Al-Si alloy, the leading eutectic Si phase is prominently grown and extends into the liquid phase, as its frequent bifurcation forms the skeleton of the eutectic group. The shape and size of the entire eutectic group are determined by the growth and branching characteristics of the leading Si phase in all directions. Under metal casting conditions, the leading phase extends in a single phase, and the eutectic group tends to be columnar, as shown in Fig. 3(a). If the leading phase grows uniformly in the anisotropy, the eutectic is spherical.

For the different eutectic regions shown in lines 1 (white) and 2 (pink), since the silicon crystals show different colors, the crystal orientations of eutectic Si are not the same, i.e., there are different crystal orientations. Both crystal defects and bifurcated growth may cause changes in the orientation of silicon crystals. Therefore, the crystallization orientation of the eutectic α in the same eutectic is obviously not the same, because the lagging eutectic α phase must adjust the growth orientation or re-nucleate growth on the silicon phase to satisfy the two phases coupling growth. This feature can be clearly seen in Figure 3(b).

Due to this feature of the eutectic, it is difficult to determine the range of eutectic clusters from the EBSD diagram. However, in the EBSD image, it can be seen

that the color of the 1 region is the same, then the orientation of the primary crystal α-Al of the 1 region and eutectic α is the same, that is, the eutectic can nucleate directly on the primary crystal. The color of the region 2 is not the same, i.e., the orientation of the α-Al of the primary crystal and the α of the eutectic are different, and the eutectic nucleus is likely to nucleate between the dendrites.

Figure 4 shows the SEM morphology and EBSD analysis of the modified AlSi10.5 alloy. From the line 1 and 2 in Fig. 4(b), it can also be seen that the eutectic nucleus is heterogeneously nucleated on the primary crystal and interdendritic. This shows that for hypoeutectic Al-Si alloys, both metamorphic and non-metamorphic eutectic nucleation exist both in primary crystals and in interdendritic heterogeneous nucleation.

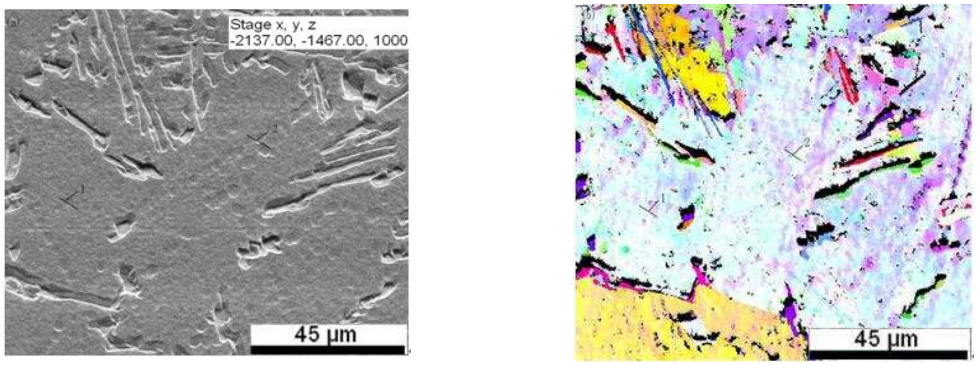

a *b*

Figure 3 – SEM&EBSD analysis of AlSi10.5 with unmodified:
a – SEM (Secondary electron); b – EBSD Mapping

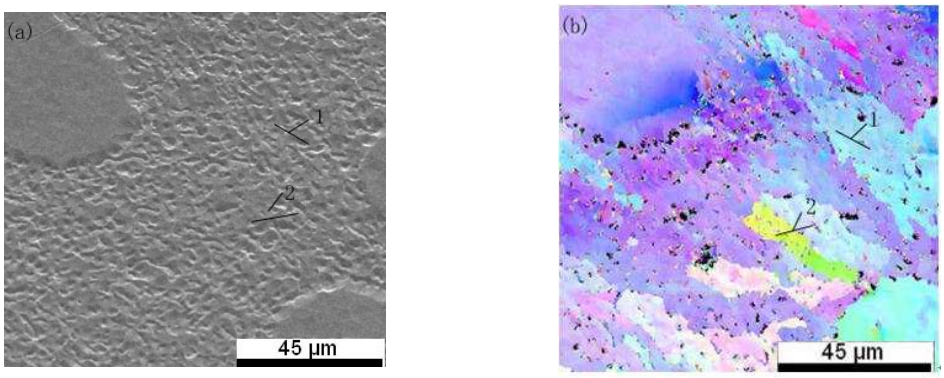

a *b*

Figure 4 – SEM&EBSD analysis of AlSi10.5 with 0.04%Sr modified:
a – SEM (Secondary electron); b – EBSD Mapping

Conclusions

1. The primary α-Al phase in the AlSi10.5 alloy modified by 0.04% Al-10 wt. % Sr is more rounded and the size is much smaller than that of the non-degraded AlSi10.5 alloy.

2. It is known through thermal analysis that the Fe-rich phase in the melt may have a large influence on the nucleation behavior of eutectic Si.

3. For hypoeutectic Al-Si alloys, eutectic nucleation exists both in primary crystals and in the interdendritic heterogeneous nucleation, both with or without deterioration.

References

1. Costa, T.A., Freitas, E.S., Dias, M., Brito, C., Cheung, N. (2015). Monotectic Al-Bi-Sn alloys directionally solidified: Effects of Bi content, growth rate and cooling rate on the microstructural evolution and hardness [J]. Journal of Alloys & Compounds, 653, 243-254.

2. Ferreira, I.L., Moutinho, D.J., Gomes, L.G., Rocha, O.L., Garcia, A. (2009). Modeling and experimental analysis of macrosegregation during transient solidification of a ternary Al-6wt%Cu–1wt%Si alloy [J]. Philosophical Magazine Letters, 89 (12), 769-777.

3. Mohamed, A.M., Samuel, F.H., Kahtani, S.A. (2012). Influence of Mg and solution heat treatment on the occurrence of incipient melting in Al-Si-Cu-Mg cast alloys [J]. Materials Science & Engineering, 543 (5), 22-34.

4. Samuel, A.M., Doty, H.W., Valtierra, S., Samuel, F.H. (2014). Relationship between tensile and impact properties in Al-Si-Cu-Mg cast alloys and their fracture mechanisms [J]. Materials & Design, 53(1), 938-946.

5. Polmear, R., Stark, J.S., Roberts, D., McMinn, A. (1990). The effects of oil pollution on Antarctic benthic diatom communities over 5 years, Marine Pollution Bulletin, 33-40.

6. Fan, J., Liu, J., Tian, S., Wu, S., Wang, S. (2015). Effect of solidification parameters on microstructural characteristics and mechanical properties of directionally solidified binary TiAl alloy [J]. Journal of Alloys & Compounds, 650, 8-14.

7. Dahle, A.K., Nogita, K., Zindel, J.K., Mcdonald, S.D., Hogan, L.M. (2001). Eutectic nucleation and growth in hypoeutectic Al-Si alloys at different strontium levels [J]. Metal and Mater Trans A, 32(4), 949−960.

8. Rocha, O.L., Siqueira, C.A., Garcia, A. (2003). Heat flow parameters affecting dendrite spacings during unsteady-state solidification of Sn-Pb and Al-Cu alloys [J]. Metallurgical and Materials Transactions A., 34 (4), 995-1006.

9. Youdelis, W.V., Dorward, R.C. (2002). Directional solidification of Al-Cu alloy in a magnetic field [J]. Canadian Journal of Physics, 44 (44), 139-150.

10. Carvalho, D.B., Guimarães, E.C., Moreira, A.L., Moutinho, D.J., Dias Filho, J.M. (2013). Characterization of the Al-3wt. % Si alloy in unsteady-state horizontal directional solidification [J]. Materials Research, 16(4), 874-883

11. Bouchard, D., Kirkaldy J.S. (1997). Prediction of dendrite arm spacings in unsteady-and steady state heat flow of unidirectionally solidified binary alloys [J]. Metallurgical and Materials Transactions B., 28 (4), 651-663.

12. Hunt, J.D., Lu, S.Z. (1996). Numerical modeling of cellular/dendritic array growth: spacing and structure predictions [J]. Metallurgical and Materials Transactions A., 27(3), 611-623.

13. Stuart, D., Kazuhiro, Nogita, Dahle, A.K. (2004). Eutectic nucleation in Al-Si alloys [J]. Acta mater, 52, 4273-4280.

14. Shankar, S., Riddle, Y.W., Makhlouf, M.M. (2004). Nucleation mechanism of the eutectic phases in aluminum-silicon hypoeutectic alloys [J]. Acta mater, 52, 4447-4460.

15. Kurtz, W. and Fisher, D.J. (1989). Fundamentals of solidification, 65.

Стаття надійшла до редколегії 03.10.2018

Рецензент: д-р техн. наук, доц. О.С.Рижков, директор ТОВ "Українсько-китайський центр шовкового шляху", Миколаїв.

Анжу Чен
Магістр техніки, напрямок досліджень: машинобудування, *orcid.org/0000-0002-6022-9793*
Яньченський політехнічний коледж, Школа автомобільної інженерії, Янчэн 224005, Китай
Пенфей Чжоу
Магістр інженерії, напрямок досліджень: матеріал з металу, *orcid.org/0000-0002-5459-9130*
Яньченський політехнічний коледж, Школа автомобільної інженерії, Яньчэн 224005, Китай;
Університет Сучжоу, школа чавуну та чавуну, Сучжоу Цзянсу 215137, Китай;
Цзянсу делонік Електромеханічні технології Лтд Цзянь Цзянсу 224731, Китай

ДОСЛІДЖЕННЯ ЕВТЕКТИЧНОЇ НУКЛЕАЦІЇ ТА МЕХАНІЗМУ РОСТУ СПЛАВУ AL-SI

Анотація. *Бінарні евтектичні перетворення Al-Si, затвердіння, що відбуваються в процесі зародження кристалів пізньої евтектики (клітини), евтектичне зародження та зростання, мають прямий вплив на формування дефектів (таких як: усадка, термічні тріщини тощо) та розподіл елементів і сполуки, домішок тощо. У цій роботі аналізу мікроструктури сплаву з модифікацією Sr, а також термічний аналіз використовували для вимірювання немодифікованих сплавів, для аналізу сплаву з різним статусом використовували EBSD. Результати показали, що: для технології EBSD, незалежно від того, модифікована чи не модифікована, ми спостерігали, що існує нуклеація евтектики на первинному дендриті та неоднорідність між дендритів, і Sr має істотний вплив на первинний α-Al, основну α-Al фазу в сплаві AlSi10,5, модифікованому 0,04% Al-10 мас. % Sr більше закруглений і має набагато менший розмірб ніж немодифікований сплав. Fe має великий вплив на зародження евтектики Si.*

Ключові слова: сплав Al-Si; EBSD; евтектична нуклеація

Link to publication

APA *Anzhu, Chen, & Pengfei, Zhou, (2018). Anzhu, Chen & Pengfei, Zhoшu (2018). The investigation of eutectic nucleation and growth mechanism of Al-Si alloy. Management of Development of Complex Systems, 36, 148 – 152.*

ДСТУ *Анжу, Чен, Пенфей, Чжоу. Дослідження евтектичної нуклеації та механізму росту сплаву Al-Si [Текст] / Анжу, Чен, Пенфей, Чжоу // Управління розвитком складних систем. – 2018. – № 36. – С. 148 – 152.*

Gu Jianhua
Master of Engineering, Associate professor in School of Mechanical and Electric Engineering,
orcid.org/0000-0002-2398-874X
School of Mechanical and Electric Engineering, Yancheng Polytechnic College, Jiangsu Yancheng 224005, P.R. China
Yan Guojun
Master of Engineering, Senior Engineer in School of Mechanical and Electric Engineering,
orcid.org/0000-0002-9169-8365
School of Mechatronic Engineering, Yancheng Polytechnic College, Jiangsu Yancheng 224005, P.R. China
Ben Nengjun
Master of Engineering, Lecturer in School of Mechanical and Electric Engineering, *orcid.org/0000-0002-3166-2985*
School of Mechatronic Engineering, Yancheng Polytechnic College, Jiangsu Yancheng 224005, P.R. China

A 12-BIT 250 MS/S SINGLE-CHANNEL PIPELINE ADC WITH 81 DB SFDR IN 0.13 UM CMOS

Abstract. *A 12bit 250-MS/s pipeline ADC is presented and fabricated in 0.13um CMOS process. A power efficient bootstrap switch with a buffer is proposed for high speed considerations. It utilizes a source follower to insulate the residue amplifier and the large capacitor in the bootstrap switch. Techniques of lightening load capacitance of each stage are proposed to speed up the corresponding residue amplifiers (RA). A clock generator and optimized timing are proposed to achieve low jitter and improve sampling linearity by saving more time for the input switch. The reference buffer and clock buffer are both fully integrated. The signal-to-distortion-and-noise-ratio (SNDR) is evaluated adopting a proper scheme and verified by the measured results. The measured SNDR is 63 dB and spurious free dynamic range (SFDR) is 81dB with 39 MHz. The core area is 2 mm^2 and the ADC consumes 160 mW at 1.3V.*

Keywords: pipeline ADC; bootstrap switches; reference buffer; clock buffer; timing

Introduction

In recent years, mobile communication systems require high performance ADCs to achieve over 80dB of SFDR at 100-300MS/s. Pipeline ADCs are the proper architecture of choice in such applications due to the balance of speed, resolution and power [1]. Time interleaved architectures have been commonly used to realize 250MS/s. However, these structures suffer from offset, gain, timing and bandwidth mismatches, which introduce spurs that limit the SFDR performance. Amplifier-sharing or capacitor-sharing is an effective way to improve the power efficiency of pipeline ADCs, however, the memory effects and cross-talk between successive stages degenerate the AC performance as well [2]. Switch-RA technique is also inadequate for high speed applications because of its turn-on time [3]. The 12 bit 250MS/s ADC in this paper is designed without the above techniques. A bootstrap switch with a buffer is proposed to save power. The load capacitance of each stage is also lightened to speed up the settling of residue voltages. A clock generator with low jitter is proposed and the timing of the ADC is optimized to improve sampling linearity. Based on PSS and Pnoise tools, the noise contributions of multiplying digital-to-analog (MDAC) and clock buffer are easily simulated. The ENOB is then easily calculated and further verified by the factual chip.

Circuit Design

ADC architecture

Fig. 1 illustrates the block diagram of the proposed ADC with a dedicated sample-and-hold amplifier (SHA), 11 pipeline stages and one 2-bit flash ADC. The flip-around S/H and 1.5bit/stage MDAC have the largest feedback factor, which is beneficial for fast settling of the residue. The ADC core works under 1.3V power supply rather than the traditional 1.2V without increasing the obvious power. The power consumption for a single-stage OTA is as the following equation [4]:

$$P \propto \frac{kT \times SNR}{\alpha V_{dd}} \quad (1)$$

When the power supply of the RA raises by 100mV, the overall power consumption decreases actually. Additionally, the switch-capacitor part contributes plenty of power consumption as well. The on-resistance of a